

VLA OBSERVATIONS OF THE $9_2-10_1A^+$ METHANOL MASERS TOWARD W3(OH)

K. M. MENTEN,¹ K. J. JOHNSTON,² T. L. WILSON,¹ C. M. WALMSLEY,¹
 R. MAUERSBERGER,¹ AND C. HENKEL¹

Received 1985 January 18; accepted 1985 March 18

ABSTRACT

Measurements at $2''$ resolution of the $9_2-10_1A^+$ emission line of methanol toward W3(OH) are presented. The frequency resolution was 12.2 kHz, or 0.16 km s^{-1} at the line rest frequency 23121.01 MHz. The two velocity components seen in single-dish spectra are separated by $\sim 1''$, but each is unresolved. This implies intrinsic source sizes of $\leq 1''$. For the masing spike feature at -43.3 km s^{-1} , the line brightness temperature is $\geq 2 \times 10^4 \text{ K}$. For the broader emission at -43.9 km s^{-1} , it is $\geq 5000 \text{ K}$, showing that this emission is also caused by masing. The spike is $0''.5$ southwest and the broader feature is $1''.5$ northwest of the continuum peak. An absorption-line spectrum of the $10_1-9_2A^-$ line taken with the 100 m telescope is also presented, and it is concluded that this absorption and the $9_2-10_1A^+$ maser emission are both formed in the same cloud where OH masers and ammonia absorption are present.

Subject headings: interstellar: molecules — masers — nebulae: H II regions — stars: formation

I. INTRODUCTION

Emission from the $9_2-10_1A^+$ transition of methanol (Wilson *et al.* 1984) was discovered toward the compact H II regions W3(OH) and NGC 7538 as well as W51 and Orion-KL. Since high-density molecular clouds for the first two sources are known to be in front of the continuum regions, the CH_3OH line emission was probably caused by masing. For the strong emission spike at -43.3 km s^{-1} toward W3(OH), the argument in favor of maser emission was convincing because of (1) the narrowness, 0.3 km s^{-1} (FWHP), of the emission spike; (2) the detection of absorption in the $10_1-9_2A^-$ line toward the compact continuum source; and (3) the intensity of the spike relative to lower J transitions in this direction. In Figure 1, we show the relevant energy levels in the A species of methanol. In order to investigate the spatial distribution of the maser spike emission toward W3(OH), and to determine whether the broader emission ($\Delta v_{1/2} = 1.6 \text{ km s}^{-1}$) centered at -43.9 km s^{-1} is also masing, we made higher resolution measurements with the Very Large Array of the NRAO.³

II. OBSERVATIONS

The observations were made in a 4 hr period on 1984 October 31. During the observations the array was in the transition from the D to the A configuration. Eighteen antennas were used with a bandwidth of 781 kHz. Sixty-four spectral channels with on-line Hanning smoothing gave a spectral resolution of 0.16 km s^{-1} , at 23121.01 MHz, the rest frequency of the $9_2-10_1A^+$ line. Observations were made

cyclically, with an 18 minute measurement of W3(OH) followed by an 8 minute measurement of 3C 84. The flux density of 3C 84 was assumed to be 43 Jy. Using this we find a continuum flux density of $2.8 \pm 0.2 \text{ Jy}$ for W3(OH), in good agreement with the estimate of Wink, Altenhoff, and Mezger (1982). The instrumental constants were established using the phases and amplitudes of the inner three-quarters of the bandwidth from the 3C 84 results. The data were analyzed using the AIPS processing system at the VLA site and the NOD2 package at the MPIfR. The 10 Jy spike at -43.3 km s^{-1} was used in the self-calibration scheme described by Schwab (1980) to calibrate the data. The maps were made with a cell size of $0''.4$, uniform weighting, and no tapering of the (uv) -plane data, in order to obtain the highest spatial resolution. The angular resolution in the resulting maps is a $2''$ circular Gaussian. The $10_1-9_2A^-$ line at 23.444 GHz (Lees *et al.* 1973) was measured using the Effelsberg 100 m telescope. The telescope, receiver, and observing details are as those in Wilson *et al.* (1984).

III. RESULTS

In order to compare the 100 m and VLA spectra of the $9_2-10_1A^+$ line, we show, in the uppermost part of Figure 2, the VLA profile obtained from an integration over a $4'' \times 4''$ region, and below, the corresponding line profile obtained with the 100 m telescope. All of the line flux density is present in the VLA data, and there is excellent agreement in the shapes of the A^+ profiles from the VLA and the 100 m dish. In the lowermost part of Figure 2, we show the $10_1-9_2A^-$ absorption line; this covers the entire velocity interval seen in the maser emission.

Our VLA maps show that the strong spike line emission at -43.3 km s^{-1} does not broaden the $2''$ beam and thus has a size of $< 1''$, after deconvolution of the synthesized beam. This is most probably also the case for the weaker emission at

¹Max-Planck-Institut für Radioastronomie.

²E. O. Hulburt Center for Space Research, Naval Research Laboratory.

³The National Radio Astronomy Observatory is operated by Associated Universities, Inc., under contract with the National Science Foundation.

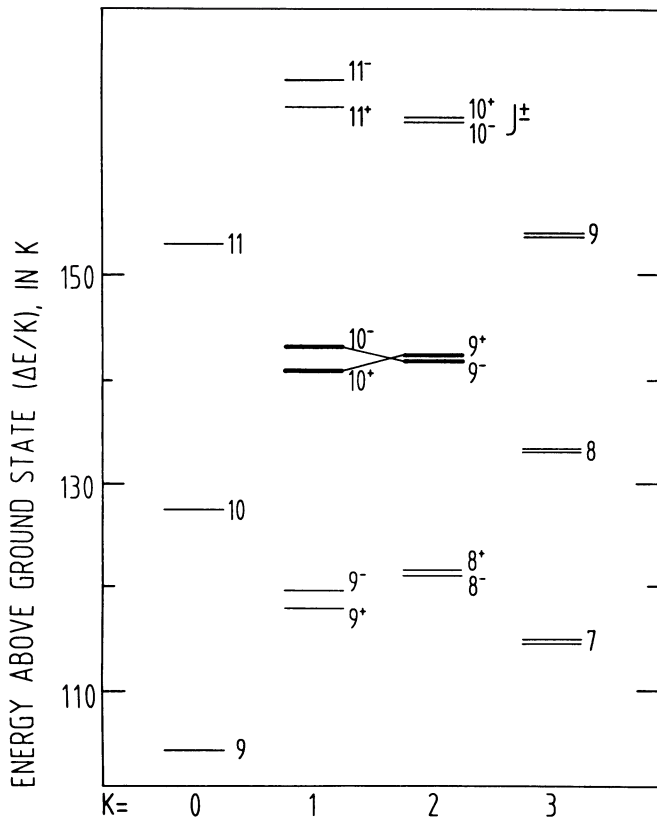


FIG. 1.—A partial energy level diagram of the A species of methanol (data from Lees *et al.* 1973).

-43.9 km s^{-1} . The size and position of the emission were measured for all channels. The positions of the strong maser line at -43.3 km s^{-1} and the continuum were established relative to 3C 84 [$\alpha(1950) = 03^{\text{h}}16^{\text{m}}29^{\text{s}}.569$, $\delta(1950) = +41^{\circ}19'51''.94$] by Gaussian fits to the appropriate channels. Because of the large angle between W3(OH) and 3C 84, the errors in our determinations are conservatively estimated to be $0''.5$. The position of the broader, weaker intensity emission centered at -43.9 km s^{-1} was determined relative to the strong maser, after self-calibration and subtraction of the continuum from the line channels. The errors in the relative positions of the spike, the broader emission, and the continuum are $0''.2$. These were obtained from the formal errors of Gaussian fits to the appropriate channels. The maser spike at -43.3 km s^{-1} is offset from the continuum by $(-0''.2, -0''.5)$, while the wider feature is offset by $(-1''.4, +0''.6)$. In Figure 3, we show the methanol centers as circles of diameter $1''$, which corresponds to the size of a point source in our beam. Our continuum peak is shown by a cross; this agrees within the errors with the centroid estimated from the higher resolution maps of Guilloteau, Stier, and Downes (1983) and Dreher and Welch (1981). The positions of the methanol emission agree with the positions of the NH_3 absorption at -44.7 km s^{-1} (Guilloteau, Stier, and Downes 1983) and with the band of OH maser spots (Reid *et al.* 1980; Norris, Booth, and Diamond 1982) toward W3(OH). The radial velocities are all in basic agreement. The size of the line emission region is $< 1''$; the line brightness temperature is $> 2 \times 10^4 \text{ K}$. This is much larger than any plausible value for the kinetic tempera-

ture and confirms the conclusion of Wilson *et al.* (1984) that the sharp spike at -43.3 km s^{-1} is due to maser emission. The presence of absorption in the $10_1-9_2A^-$ transition implies that the cloud containing methanol is in front of the continuum source. If so, the $\sim 1000 \text{ K}$ continuum temperature of the background source is amplified, and the peak optical depth is > 3 . This is a limit, since the masing region could be smaller. The wider, weaker emission feature centered at $\nu = -43.9 \text{ km s}^{-1}$ is also due to maser emission, since the observed peak T_B of this feature, from the VLA data, is $> 5000 \text{ K}$. The inversion of the $9_2-10_1A^+$ transition, together with the absorption detected in the $10_1-9_2A^-$ line, is most simply explained by an overpopulation in the 9_2 relative to the 10_1 level (see Fig. 1). Then the methanol amplifies the background continuum radiation in the $9_2-10_1A^+$ line and absorbs it in the $10_1-9_2A^-$ transition. This suggests that the $K=2$ stack is overpopulated relative to the $K=1$, and one might expect, for example, that the $8_2-9_1A^-$ at 28.97 GHz should also be masing.

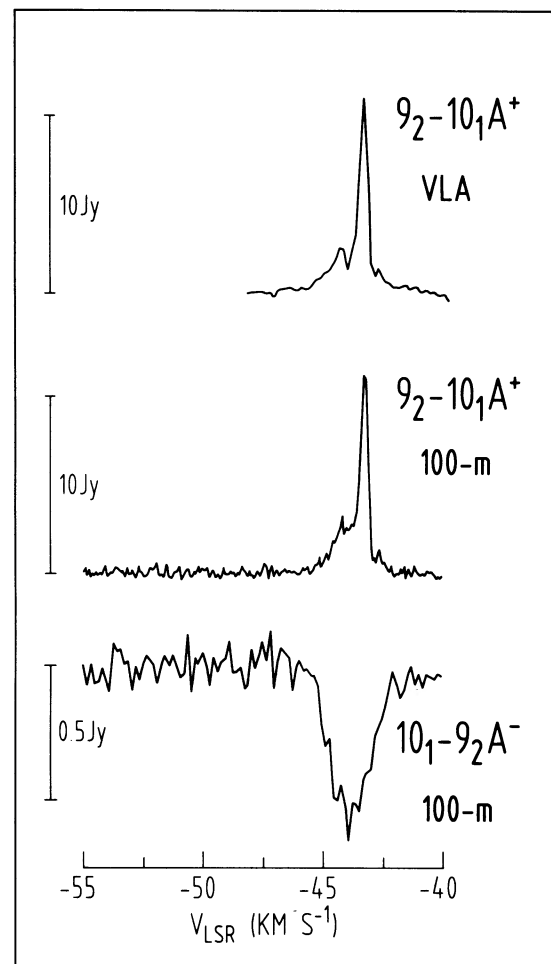


FIG. 2.—On top is a VLA spectrum of the $9_2-10_1A^+$ line, averaged over a $4'' \times 4''$ region. Below are 100 m spectra of the $9_2-10_1A^+$ and $10_1-9_2A^-$ lines, taken with a $40''$ beam toward W3(OH). The velocity resolution of the VLA spectrum is 12.2 kHz or 0.16 km s^{-1} . The rest frequency of the $9_2-10_1A^+$ line is 23121.01 MHz , and that of the $10_1-9_2A^-$ line is 23444.82 MHz (Lees *et al.* 1973). The velocity resolutions of the 100 m spectra are 0.04 km s^{-1} (for A^+) and 0.16 km s^{-1} (for A^-).

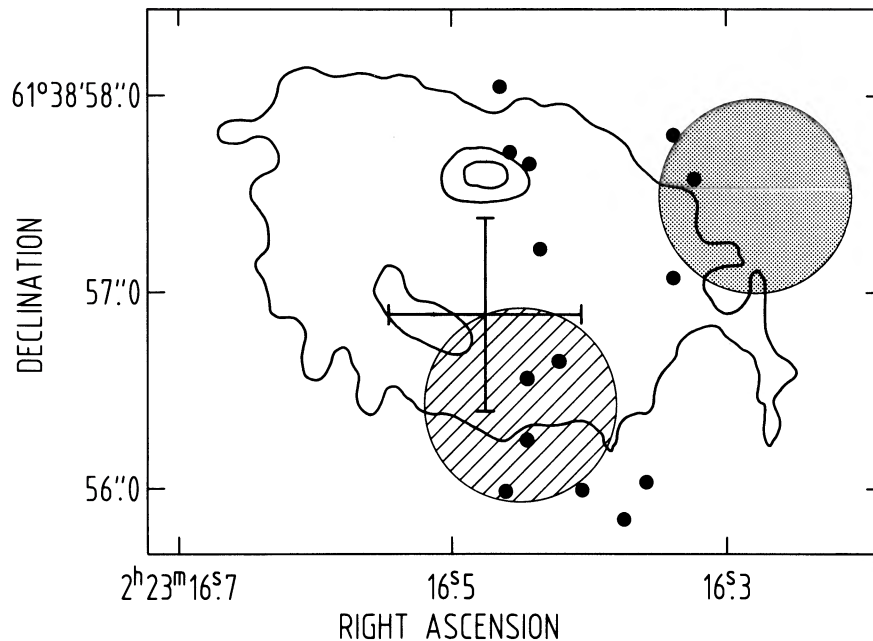


FIG. 3.—The positions of the two $9_2-10_1 A^+$ methanol masers, shown as hatched (-43.3 km s^{-1} spike) and shaded (-43.9 km s^{-1} feature) circles of diameter $1''$, superposed on the lowest (175 K), the 2450 K, and 3150 K contours from the 23 GHz VLA continuum map of Guilloteau *et al.* (1983). The center of our continuum emission [$\alpha(1950) = 02^{\text{h}}23^{\text{m}}16^{\text{s}}.48$, $\delta(1950) = +61^{\circ}38'56''.9$] is shown by a cross. The spots show the positions of 18 cm OH masers (Reid *et al.* 1980). The relative positions of the CH_3OH masers and the continuum are accurate to $0''.2$. The absolute positions are uncertain by $0''.5$.

Provided that all of the $9_2-10_1 A^+$ emission arises from gas in front of W3(OH), the difference between the shapes of the A^+ and A^- spectra in Figure 2 are caused mostly by the emission spike at -43.3 km s^{-1} . This could be explained if there is a long path in the methanol cloud at -43 km s^{-1} in which there is only a very small velocity gradient in our direction. This allows a buildup of the line intensity. Depending on the distance between the H II region and the molecular cloud, the radiation from the A^+ emission spike could be highly beamed. For the $10_1-9_2 A^-$ transition, we assume that the cloud parameters are the same, but that deviations from LTE are in the opposite sense and lead to absorption of the background radiation. If, as in the A^+ maser spike, the optical depth in the A^- line is > 2 , the methanol at this radial velocity covers only 11% of the continuum source. Taking the optical depth of the $10_1-9_2 A^-$ line as 2, assuming that the excitation and rotation temperatures are 100 K (similar to the values obtained from NH_3 ; Pauls and Wilson 1980), we obtain a total methanol column density of $\sim 2 \times 10^{18} \text{ cm}^{-2}$ and a space density of $\sim 10^2 \text{ cm}^{-3}$. These estimates depend

strongly on the assumed excitation temperature. If the physical conditions are similar to those in the NH_3 and OH region, the H_2 density would be $\sim 10^7 \text{ cm}^{-3}$ and the column density $\sim 10^{23} \text{ cm}^{-2}$ in the methanol line formation region (see, e.g., Guilloteau, Stier, and Downes 1983). Then the $(\text{CH}_3\text{OH}/\text{H}_2)$ ratio is $\sim 10^{-5}$, which is ~ 100 times the typical value (see, e.g., Watson and Walmsley 1982). Such high methanol abundances have consequences for models of E type J_2-J_1 CH_3OH masers (see Strel'nitskii 1981). It seems likely to favor pump schemes involving radiative excitation of vibrational transitions. The phenomenon of overabundance close to a compact H II region is reminiscent of ammonia, which is also overabundant in molecular clouds near compact H II regions (see the discussion in Wilson *et al.* 1983). Mauersberger *et al.* (1984) point out that this may be related to elevated grain temperatures in such regions, since temperatures above $\sim 70 \text{ K}$ probably allow the evaporation of icy mantles.

This work is supported in part by NATO grant 731/84.

REFERENCES

- Dreher, J. W., and Welch, W. J. 1981, *Ap. J.*, **245**, 857.
 Guilloteau, S., Stier, M. T., and Downes, D. 1983, *Astr. Ap.*, **126**, 10.
 Lees, R. M., Lovas, F. J., Kirchhoff, W. H., and Johnson, D. R. 1973, *J. Phys. Chem. Ref. Data*, **2**, 205.
 Mauersberger, R., Wilson, T. L., Batrla, W., Walmsley, C. M., and Henkel, C. 1984, *Astr. Ap.*, in press.
 Norris, R. P., Booth, R. S., and Diamond, P. J. 1982, *M.N.R.A.S.*, **201**, 209.
 Pauls, T. A., and Wilson, T. L. 1980, *Astr. Ap.*, **91**, L11.
 Reid, M. J., Haschick, A. D., Burke, B. F., Moran, J. M., Johnston, K. J., and Swenson, G. W. 1980, *Ap. J.*, **239**, 89.
 Schwab, F. R. 1980, *Proc. Soc. Photo-Opt. Instrum. Eng.*, **231**, 18.
 Strel'nitskii, V. S. 1981, *Soviet Astr. Letters*, **7**, 223.
 Watson, W. D., and Walmsley, C. M. 1982, in *Regions of Recent Star Formation*, ed. R. S. Roger and P. E. Dewdney (Dordrecht: Reidel), p. 357.
 Wilson, T. L., Mauersberger, R., Walmsley, C. M., and Batrla, W. 1983, *Astr. Ap.*, **127**, L19.
 Wilson, T. L., Walmsley, C. M., Snyder, L. E., and Jewell, P. R. 1984, *Astr. Ap.*, **134**, L7.
 Wink, J., Altenhoff, W. J., and Mezger, P. G. 1982, *Astr. Ap.*, **108**, 227.

C. HENKEL, R. MAUERSBERGER, K. M. MENTEN, C. M. WALMSLEY, and T. L. WILSON: Max-Planck-Institut für Radioastronomie, Auf dem Hügel 69, 5300 Bonn, Federal Republic of Germany

K. J. JOHNSTON: E. O. Hulburt Center for Space Research, Naval Research Laboratory, Washington, DC 20375-5000

© American Astronomical Society • Provided by the NASA Astrophysics Data System